Influence of Conformational Asymmetries on Local Packing and Small-Angle Scattering in Athermal Diblock Copolymer Melts

Edwin F. David and Kenneth S. Schweizer*

Departments of Chemistry, Materials Science & Engineering, and Materials Research Laboratory, University of Illinois, 1304 West Green Street, Urbana, Illinois 61801

Received November 11, 1994; Revised Manuscript Received February 24, 1995®

ABSTRACT: Local structural correlations and small-angle scattering profiles are studied using the polymer reference interaction site model (PRISM) integral equation theory for a series of structurally asymmetric diblock copolymer melts in the athermal limit. Motivated by recent experimental work on polyolefin and polydiene copolymers, we have chosen the block aspect ratios and the overall degree of copolymer asymmetry to be representative of those systems. The extent of nonrandom mixing in the fluid is quantified by calculating length scale dependent "effective compositions". These deviations from the bulk composition in the athermal fluid are compared to those of a fully interacting thermal system. The athermal contribution to nonrandom mixing, resulting from pure stiffness asymmetry, is quite small relative to the effects brought on by unfavorable enthalpic AB interactions. Nonetheless, deviations from random mixing in the athermal limit can lead to appreciable unfavorable enthalpic interactions between components within a thermodynamic perturbative scheme. Large departures from the widely assumed equality of the three partial collective structure factors are also found, suggesting that the extraction of a single χ parameter by fitting to a form which assumes incompressibility may in some cases be unreliable.

I. Introduction

During the past decade significant progress has been made toward the understanding of the phase behavior of diblock copolymer melts.[1,2] For weakly segregated systems, the original theoretical work of Leibler[3] is still used as a basis for extracting information about the phase stability of block copolymers in much the same way as the Flory−Huggins theory is employed to determine χ parameters in polymer blends. Since then, several workers have put forth theories which treat architectures beyond the symmetric diblock,[4−10] fluctuation corrections,[11−17] compressibility effects,[5,16,18,19] the structure and stabilities of complicated new ordered phases,[20,21] and the intermediate segregation regime.[15,22] These more sophisticated descriptions of block copolymer thermodynamics are required for experimentally realistic systems since most copolymers have some degree of asymmetry in composition, structure, and/or interaction.[23−30] Moreover, the degree to which nonzero compressibility affects macroscopic observables as a general function of copolymer asymmetry, backbone stiffness, molecular weight, and melt density is still largely unknown.

Recently, many hydrocarbon blend and diblock copolymer melts have been experimentally studied which have what are believed to be very small differences in the attractive dispersion interactions between components (small χ_o, where χ_o, is the Flory *mean field* enthalpic interaction parameter) but possess different monomer architectures.[26,30,31] These experiments suggest that the structural disparity between components can influence the phase behavior significantly, despite the fact that the monomeric units which make up the chains are nearly chemically identical. One of the most striking examples of this is the saturated polyolefins which consist entirely of carbon and hydrogen and often have identical chemical formulas. In these polymers structural asymmetries are generated as a result of the type and amount of branching which exists along the chain backbone. Since the mean field energetic driving force for segregation in these systems is small, it is reasonable to assume that their phase behavior is strongly influenced by structural disparity. In particular, the efficiency with which different olefin blocks *locally* pack is expected to be an important consideration. The primary issue which we shall address in this paper is the influence of backbone structural asymmetry on both the local and nonlocal structure, and the small-angle scattering profiles, in the disordered melt. The continuous space description which the polymer reference interaction site model (PRISM) integral equation theory of block copolymers[17] provides is well suited for these questions relating to local packing and compressibility effects.

We also note that although the net enthalpic interactions are small in these systems, there is no theoretical justification for treating them as purely "athermal". That is, despite the fact that the real attractive interactions may nearly "cancel" in a mean sense (i.e. $\chi_o \approx 0$), their very presence is what presumably gives rise to thermally induced, molecular weight dependent order−disorder transitions (ODT). Nonetheless, within the approximate van der Waals picture of dense fluids, the structural features of the fully interacting thermal system are largely determined by the repulsive ("athermal") branch of the intermolecular potential. Furthermore, since integral equation calculations of fully interacting melts require as input the intermolecular correlations in the athermal "reference system",[17] it is useful to fully characterize the repulsive force copolymer fluid. Understanding the properties of the athermal melts of structurally asymmetric copolymers provides a starting point from which their thermodynamic properties can be studied. In particular, within *perturbative*, free energy based approaches to predicing the *thermal* effective χ parameters and ODT temperatures, it is only the athermal structural correlations which are relevant. Using incompressible field theoretic methods, Fredrickson et al.[9] have also developed a theory of athermal, conformationally asymmetric polymer alloys. In their study, thermal effects enter only implicitly through the (experimentally determined) temperature dependence

® Abstract published in *Advance ACS Abstracts,* April 15, 1995.

0024-9297/95/2228-3980$09.00/0

of the statistical segment lengths (and hence conformational mismatch) and density.[9]

The primary goal of the present paper is to establish the role of pure packing effects in the athermal limit, which has been the subject of recent discussions and some controversy. We also estimate the relative magnitudes of the athermal versus thermal contributions to the effective χ parameter. One of our major conclusions is that melts composed of *flexible* diblocks, with block aspect ratios representative of those found in the olefin- and diene-based copolymers, are *not* close to the stability limit when only athermal packing is considered. That is, we find explicit thermal interactions must be introduced in order to drive the system close to a microphase boundary. These conclusions hold at least for the finite N, linear semiflexible chain models studied here. Thus, for the *athermal model* the issue of long wavelength concentration fluctuation effects associated with the ODT is not of central importance. Detailed experimental applications, and the effect of thermally-driven concentration fluctuations in asymmetric diblock fluids, will be addressed in future work.

The remainder of this paper is organized as follows. In section II we outline the integral equation theory for block copolymers,[17] and define the quantities which are calculated. The asymmetric diblock model is presented in section III. Section IV presents results for the small wavevector partial collective structure factors. Predictions for the asymmetry, chain length, and composition dependencies of the local and nonlocal structure are given in section V. Perturbative estimates for thermal properties of the asymmetric diblock melts are discussed in section VI. A summary and conclusions are given in section VII. The Appendix contains a brief description of the discrete semiflexible chain model used in our calculations.

II. Theory

A. Integral Equation Theory. Polymer RISM (PRISM) integral equation theory[32-34] describes the average *inter*molecular pair distribution functions, $g_{MM'}(r)$, between two "interaction sites" of type M and M′ which interact through a spherically symmetric pair potential $v_{MM'}(r)$. These sites can represent either elementary repeat units such as a methylene group or some collection of these which may constitute a coarse-grained "segment". A tractable theory requires the intermolecular pair distribution functions to be taken as species dependent only, *not* dependent on where along the block a particular site is (e.g. close to the junction or near a chain end, etc.).[17] Of course, the junction is explicitly treated in the theory through the intramolecular distribution functions. The block-averaging approximation is best for large diblocks and for strictly alternating (i.e. ABAB...) copolymers.

To calculate the pair correlation functions, one first specifies the single chain structure factor through an intramolecular probability distribution matrix $\hat{\Omega}$ defined by

$$\hat{\Omega}_{MM'}(k) \equiv \varrho \sum_{\alpha=1}^{N_M} \sum_{\gamma=1}^{N_{M'}} \hat{\omega}_{\alpha M \gamma M'}(k) \qquad (2.1)$$

where $\hat{\omega}_{\alpha M \gamma M'}(k)$ are the Fourier-transformed normalized probability densities of finding sites α and γ of species M and M′, respectively, on the *same* chain separated by a distance r, N_M is the number of sites of type M on a single copolymer chain, and ϱ is the number density of copolymers. With $H_{MM'}(r) \equiv \varrho_M \varrho_{M'}[g_{MM'}(r) - 1]$, where $\varrho_M = N_M \varrho$, the block-averaged intermolecular correlation function matrix can be written in Fourier space as[17,32]

$$\hat{\mathbf{H}} = [\mathbf{1} - \hat{\mathbf{\Omega}}\hat{\mathbf{C}}]^{-1}\hat{\mathbf{\Omega}}\hat{\mathbf{C}}\hat{\mathbf{\Omega}} \qquad (2.2)$$

where we have dropped the wavevector argument for notational simplicity and the functions $\hat{C}_{MM'}(k)$ are the site−site direct correlation functions. Equation 2.2 corresponds to decomposing the total intermolecular correlation functions into linear sequences of elementary intramolecular ($\mathbf{\Omega}$) and intermolecular ($\mathbf{C}$) correlation pathways.[32] If $\hat{\Omega}$ is assumed to be independent of intermolecular structure (rigorously true for rigid molecules with no internal degrees of freedom), then eq 2.2 can be solved with another "closure" relation for $C_{MM'}(r)$. For athermal systems the site−site analog to the Percus−Yevick closure for atomic fluids is employed[32,35]

$$C_{MM'}(r) = 0 \qquad r > d_{MM'}$$
$$g_{MM'}(r) = 0 \qquad r < d_{MM'} \qquad (2.3)$$

where $d_{MM'}$ is the distance of closest approach between sites M and M′. Note that the first relation is approximate while the second is exact for molecules consisting of spherically symmetric, impenetrable sites. The solution of eq 2.2 with eqs 2.1 and 2.3 yields the intermolecular correlation functions for an athermal diblock fluid, given the matrix $\mathbf{\Omega}$ which specifies the copolymer architecture.

Note that, in general, the intramolecular distribution functions depend in a nontrivial way on the *inter*molecular fluid structure [$g_{MM'}(r)$]. This self-consistent interdependence or coupling of the inter- and intramolecular correlation functions has been addressed by several workers within the chain molecule,[36] polymer,[37] and quantum electron[38] liquid state approaches but is beyond the scope of this paper. For the athermal, dense melts which are the focus of our present study we invoke the Flory *ansatz* that the intrachain structure remains ideal. Explicit forms for $\mathbf{\Omega}$ are discussed in section III.

B. Collective Structure Factors and Intermolecular Correlation Functions. Our discussion of athermal results shall be separated into two parts: (i) small-angle collective scattering profiles (section IV) and (ii) interchain structural correlations (section V). The first property is related to the overall stability of the fluid against microphase separation, and the second describes how molecules organize relative to each other on length scales on the order of the range of intermolecular interactions and beyond. Of course these two questions are related since the packing efficiency of asymmetric copolymers is expected to change the overall stability of the fluid.

The angularly averaged scattering profiles, or species-dependent density−density fluctuation correlation functions, are defined by

$$\hat{S}_{MM'}(k) = \int d(\mathbf{r} - \mathbf{r}')\, e^{i\vec{k}\cdot(\mathbf{r}-\mathbf{r}')} \langle [\varrho_M - \varrho_M(\mathbf{r})][\varrho_{M'} - \varrho_{M'}(\mathbf{r}')] \rangle \qquad (2.4)$$

where $\varrho_M(\mathbf{r})$ is the number density of sites of species M at position $\mathbf{r}$ and the angled brackets denote an equilibrium ensemble average. These are conveniently calculated from the inter- and intramolecular structure factor matrices,

$$\hat{\mathbf{S}} = \hat{\mathbf{\Omega}} + \hat{\mathbf{H}} = \hat{\mathbf{\Omega}}^{-1} - \hat{\mathbf{C}} \tag{2.5}$$

Within a theory for compressible diblock fluids this quantity is a matrix composed of three distinct partial structure factors. Only for the idealized case of a dense, structurally and interaction symmetric diblock fluid is the reduction of the three partial structure factors to one unique structure factor, by invoking incompressibility, expected to be a reliable approximation.[16,39] As we will discuss, the degree to which the three partial structure factors differ is highly dependent on block asymmetry.

A quantity which is deducible from the pair distribution functions, but is perhaps more intuitive, is the effective composition, $\Phi_{MM'}(R)$. This is defined to be the composition of component M′ in a sphere of radius R centered about a site of type M. In terms of the radial distribution functions, the length scale dependent compositions are defined as[40]

$$\Phi_{MM'}(R) = \frac{\int_0^R \mathrm{d}r\, 4\pi r^2 \varrho_M g_{MM'}(r)}{\sum_{M''} \int_0^R \mathrm{d}r\, 4\pi r^2 \varrho_{M''} g_{MM''}(r)} \tag{2.6}$$

It is important to note that these effective composition variables differ from the *one-body* composition fields usually discussed in the context of block copolymer field theories. The quantities of eq 2.6 are related to *two-point intermolecular* distribution functions and describe the composition associated with different chains in a given region of space about a reference site on a tagged chain. In the thermodynamic limit of $R \to \infty$, or the random mixing limit of $g_{MM'}(r) \approx g(r)$ for all M and M′, the effective composition becomes the volume fraction of species M (i.e. $\Phi_{MM} = f_M$, for the case of equal site volumes on the two blocks).

One motivation for defining such a two-point quantity comes from dynamical measurements which probe *inter*chain interactions and friction. In recent years effective local compositions have been discussed in the interpretation of dynamical measurements on copolymer and blend systems. Although a direct measurement of this quantity is not possible with present techniques, model-dependent attempts to extract such information have been made by several groups.[41-45] Depending on which experimental probe is used, the value of R (i.e. the so-called "correlation radius") might be close in magnitude to the monomer size or the block size for nuclear magnetic resonance (NMR) and dielectric spectroscopy (DES) probes, respectively. Of course, small-angle scattering corresponds to probing the $R \approx D$ effective composition, where D is the microphase domain size. We also note that our definition gives only the *inter*molecular contribution to the length scale dependent composition, which is particularly relevant for dynamic questions since condensed phase effective friction coefficients arise from interchain processes. The "absolute" effective composition can be calculated by including the trivial intramolecular contribution as well (i.e. $\Omega_{MM'}$).

Another quantity which is a useful real space measure of species segregation, or "clustering", in the fluid is the difference correlation function

$$\Delta g(r) \equiv \frac{g_{AA}(r) + g_{BB}(r)}{2} - g_{AB}(r) \tag{2.7}$$

which is identically zero for random mixing but generally varies as a function of the structural disparity between blocks. A non-zero $\Delta g(r)$ can be interpreted as follows:

$$\Delta g(r) > 0 \;\Rightarrow\; \text{like species pairing favored at } r \tag{2.8}$$

$$\Delta g(r) < 0 \;\Rightarrow\; \text{unlike species pairing favored at } r \tag{2.9}$$

As discussed previously, even for structurally symmetric models, this function gradually grows in amplitude and develops R_g scale oscillations as the diblock melt is cooled toward microphase separation.[17] Here, however, we study how this correlation function depends on block structural disparity in the athermal limit.

C. Effective Thermal Interactions. Related to $\Delta g(r)$ (for certain choices of interactions), and a measure of the energetic consequences of nonrandom mixing on local length scales, is what we call a dimensionless "exchange energy", $\Delta\bar{E}$, defined by

$$\Delta\bar{E} \equiv -\frac{\beta\varrho_m}{2}\int \mathbf{dr}\,[v_{AA}(r)g_{AA}(r) + v_{BB}(r)g_{BB}(r) - 2v_{AB}(r)g_{AB}(r)] \tag{2.10}$$

where $\varrho_m \equiv \varrho_A + \varrho_B$ is the total site number density and $\beta = 1/k_BT$, k_B being the Boltzmann constant. In simple Flory theory one approximates $g_{MM'}(r) \approx 1$ and $\Delta\bar{E}$ becomes the off-lattice mean field, or bare, chi parameter χ_o. For the olefins (and also dienes), we expect the "bare" interactions $v_{MM'}(r)$ to be nearly equivalent. In this idealized case of "complete interaction symmetry" $v_{MM}(r) \equiv v(r)$, and by choosing a shifted Lennard-Jones-like attractive tail interaction for $v(r)$, eq 2.10 becomes

$$\Delta\bar{E} = -\varrho_m\beta\epsilon\int \mathbf{dr}\left[\left(\frac{d}{r}\right)^{12} - 2\left(\frac{d}{r}\right)^{6}\right]\Delta g(r) \tag{2.11}$$

where $\epsilon > 0$ is the attractive well depth at the distance of closest approach. The specific copolymer model we shall study here consists of equal hard-core diameter blocks, and hence $d_{MM'} \equiv d$ in eq 2.11. Structural asymmetries are then treated by introducing different backbone bending energies or persistence lengths. Absolute magnitudes for $\Delta\bar{E}$ can be determined for olefins by estimating the potential well depth for two interacting methylene units. Since $\Delta\bar{E}$ weights most strongly $\Delta g(r)$ on the length scale of the interactions, it is a single energetic measure of the magnitude of *local* nonrandom mixing. We also note that within thermodynamic perturbation theory of polymer *blends*, this quantity is one of the contributions to the enthalpic part of the effective χ parameter.[46] In fact, if one assumes constant volume conditions *and* neglects the composition dependence of the athermal pair correlation functions, then $\Delta\bar{E}$ is precisely the thermal χ parameter as defined by $2\chi_{eff} = -\partial^2\Delta H_m/\partial\phi^2$, where ΔH_m is the enthalpy of mixing for a polymer blend and ϕ is the mixture composition variable.

The relationship of $\Delta\bar{E}$ to a χ parameter in the case of block copolymers is much less clear. This stems from the fact that the diblock melt is a one-component fluid in the thermodynamic sense, and hence the compositional variable f cannot be treated in direct analogy with the blend ϕ. In blends, a change in ϕ corresponds to mixing different mole fractions of the two chains. In

contrast, changing f requires changing the block *size* in a copolymer (which in some sense is more akin to a change in the actual architecture). Despite these issues, it is of interest to define a "heat of mixing", δH, for the copolymer fluid. We use the symbol δH rather than ΔH because this quantity should not be literally interpreted as a heat of mixing. Rather it is the difference in enthalpy of the disordered, or "mixed", diblock fluid with that of the hypothetical disconnected pure component system, in analogy to the blend. However, an "enthalpy of ordering" would require subtracting the enthalpy of the ordered structure from the disordered phase enthalpy and hence would require a theory for the inhomogeneous phases.

The enthalpy per unit volume associated with *inter*-chain interactions of the copolymer fluid, H_{cop}, is given by

$$\varrho_m H_{cop} \equiv \frac{1}{2}\sum_{M,M'} \int \mathbf{dr}\, \varrho_M \varrho_{M'} v_{MM'}(r) g_{MM'}(r) \quad (2.12)$$

In the high-temperature perturbative limit, the structural correlations $g_{MM'}(r)$ are taken to be those in the athermal fluid. Using $v_{MM'}(r) = v(r)$ as in eq 2.11 and subtracting off the pure component enthalpies from H_{cop} give the "heat of mixing" as

$$2\varrho_m^{-1}\delta H = \int \mathbf{dr}\, v(r)[f^2 g_{AA}(r) + (1-f)^2 g_{BB}(r) + 2f(1-f)g_{AB}(r) - f g_A^{(m)}(r) - (1-f) g_B^{(m)}(r)] \quad (2.13)$$

where $\varrho_A = f\varrho_m$ and $g_M^{(m)}(r)$ is the homopolymer melt pair correlation function for species M. Although there is no rigorous connection between δH and a χ parameter, it is of some interest to investigate the degree to which there might be a correlation between the Flory-like quantity $\chi_H \equiv \varrho_m^{-1}\delta H/f(1-f)$, and the second derivative $-\varrho_m^{-1}\partial^2\delta H/2\partial f^2$. As we will show, there is reasonable consistency between this second derivative quantity and the enthalpic "χ parameter", χ_H.

III. Chain Models and Mappings

A. Asymmetric Diblock Copolymers. Structural asymmetries in real copolymers arise for a variety of different reasons. In many molecules the monomers composing the blocks can have different shapes and effective collision diameters. Even if monomers are represented as spherical objects, when strung together to form a linear chain the result is a copolymer in which the block backbones vary in overall "thickness". Blocks may also possess a "stiffness" asymmetry due to variations in bond bending and torsional energies, and in the liquid state these are influenced by the surrounding molecules.[36,37] Many hydrocarbon copolymers of commercial interest have the same basic backbone structure (*e.g.* carbon−carbon bonds) but have varying degrees of branching off the backbone. Systems which have been widely studied in both the blend and block copolymer varieties are the polyolefins and polydienes wherein the (short) branches or side groups also consist of simple hydrocarbon units. Because of the commercial importance of these materials, and mixtures thereof, many types of experiments have been carried out in an attempt to understand the effects of backbone stiffness and side chain branching.[26,27,30,31] Recent attempts to correlate the phase behavior of polyolefin alloys based on pure component data have also been fairly successful.[31] This suggests that "calibrating" the properties of the diblock theoretical model (e.g. the aspect ratios of the blocks) based on homopolymer melt data may in some cases be sufficient for predicting the stabilities of the alloys which they compose.[47] This is a common idea which underlies the solubility parameter and related approaches.

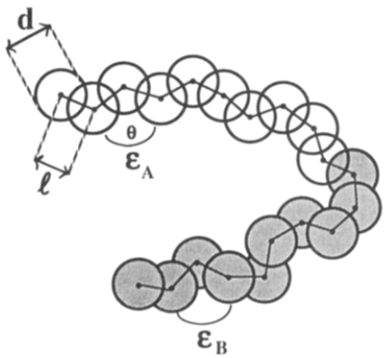

Figure 1. Schematic representation of the semiflexible diblock model. The structure of any one block of species M is characterized by a bond length, l_M, a hard-core diameter d_M, and a local bending energy $E_{b,M} = \epsilon_{b,M}(1 + \cos\theta)$. Shown is the case for $d_A = d_B \equiv d$ and $l_A = l_B \equiv l$ which is used in this work.

Because real copolymers exhibit so many types of asymmetry in structure, it is difficult to know how to map such copolymers onto a coarse-grained model. Given a certain "class" of structurally asymmetric copolymer (e.g. stiffness asymmetric, monomer volume asymmetric, etc.), one may be able to construct a tractable and representative coarse-grained model. Although one can always "map" any polymer onto a coarse-grained Gaussian model by defining a statistical segment, there is no reason to expect that after having done so the structural correlations and thermodynamic properties in the melt will be faithfully described. Since the number of different *types* of asymmetry in blends and copolymers is relatively small, these intermediate level coarse-grained descriptions provide some hope for extracting general trends in alloy behavior within a homologous series of materials without doing atomistic level calculations (simulation or otherwise) on a case by case basis.[47]

B. Discrete Semiflexible Diblock. We choose the discrete Koyama semiflexible model[48] for the intramolecular distribution functions $\Omega_{MM'}$. This model consists of a linear sequence of hard beads, as shown in Figure 1, all having diameter d and separated by bonds of fixed length l. Additionally, there are two bond bending energies, $\epsilon_{b,A}$ and $\epsilon_{b,B}$, that are used to tune the stiffness of the backbone within each block. Note that this model is a "pure stiffness asymmetric" model in that we have set the site hard-core diameters (block thickness) to be equal. Therefore, to "map" a real polymer onto this model, it must be done on an equal volume basis. In this sense, our modeling of stiffness is similar in spirit to previous work in which chain stiffness is accounted for on an equal volume basis.[9,16,47] Details of this model are furnished in the Appendix. As discussed at length elsewhere[47] it is important to determine, in an *absolute* sense, what the relevant range of aspect ratios (on an equal repeat unit diameter basis) is for the specific polymers of interest. In terms of the chain parameters, the aspect ratio of species M is defined as $\Gamma_M \equiv \sigma_M/d$, where σ_M is the statistical segment length (i.e. $\sigma_M^2 \equiv 6R_{g,M}^2/N$) and d is the repeat unit hard-core diameter. "Calibration" of the single chain aspect ratios for realistic flexible polymers,

Table 1. Aspect Ratios, $\Gamma_M \equiv \sigma_M/d$, of the Blocks Which Compose the Semiflexible Copolymers (A–D) in This Study[a]

copolymer	Γ_A	Γ_B	$\gamma \equiv \Gamma_B/\Gamma_A$	$R_{g,A}$	$R_{g,B}$	$D \equiv 2\pi/k^*$
A	1	4/5	4/5	6.383	5.131	26.3
B	1	1	1	6.383	6.383	29.2
C	1	5/4	5/4	6.383	7.924	32.8
D	1	3/2	3/2	6.383	9.430	36.6

[a] σ_M and d are the statistical segment length of species M and hard-core diameter $d_M \equiv d$, respectively. Also listed in units of the hard-core diameter are the A- and B-block radii of gyration and D, the microdomain size for the $f = 0.5$, $N = 500$ copolymers studied in Figures 3–7.

and how the chain statistics affect bulk properties such as cohesive energy density, have been discussed elsewhere.[47] In short, there is a strong correlation between the degree of backbone branching and the average efficiency with which the monomer units can pack. Generally, as the overall degree of branching increases and/or the backbone characteristic ratio decreases the absolute magnitude of the cohesive energy of the system is lower due to a decreased number of intermolecular contacts,[47] i.e. a smaller local $g(r)$. Although exceptions do exist, our prior work suggests the combined effects of variable branching and backbone stiffness can be usefully mimicked by using an effective unbranched chain.[47]

To determine the bond bending energy, and hence the effective stiffness, which corresponds to a particular choice of aspect ratio Γ, we equate the end-to-end distance of a Gaussian chain having statistical segment length σ to that of a semiflexible chain having a certain average bond angle (determined by the bending energy ϵ_b),

$$N\sigma^2 = Nl^2\left(\frac{2}{1 + \langle\cos\theta\rangle} - 1\right) \tag{3.1}$$

where the right-hand side of eq 3.1 is an implicit function of bending energy ($\langle\cos\theta\rangle$ is given explicitly in terms of the bending energy in ref 48). Division of both sides by the square of the hard-core diameter d and using the definition of aspect ratio $\Gamma \equiv \sigma/d$ one finds

$$\langle\cos\theta\rangle = \frac{2}{1 + (d/l)^2\Gamma^2} - 1 \tag{3.2}$$

For a particular choice of l/d and aspect ratio Γ, a bond bending energy can be computed to yield $\langle\cos\theta\rangle$ which solves eq 3.2. For the asymmetric diblock each block will have a different Γ. Table 1 lists the four model copolymers which we will present results for. Note that although the aspect ratio and the ratio of these are specified, there are many possible choices for l/d (the degree of overlap between adjacent segments). We have chosen an aspect ratio of $\Gamma = 1$ for the "common block" and vary the B-block such that case A and C have the same ratio, but case C has a larger overall stiffness. Case D has $\gamma = 3/2$, and we consider this to be an extreme asymmetry in the context of real hydrocarbons such as polyolefins and polydienes. In all, our common block aspect ratio, and those chosen for the variable B-block, are believed to roughly cover the range of both average stiffness and stiffness disparity in both the olefin and diene series.[47] (The low and high extremes in olefin series are poly(ethylethylene) (PEE) and polyethylene (PE), respectively.) This statement is based on comparison of homopolymer melt calculations to *PVT* data and solubility parameters of the pure components[31,47] or direct estimation of the segment length on an equal volume basis.[30] We also note that Gehlsen and Bates[30] have recently studied saturated hydrocarbon polymers in which they hold the microstructure of one "common" block (polyvinylcyclohexane) fixed, while varying the properties of the other.

C. Calibration of Melt Density. Although compressible PRISM theory is applicable over the entire range in density, we limit our study here to meltlike densities.[49] In order to determine the density at which to carry out calculations we have performed a "calibration" procedure.[16,17,47] The goal is to choose a real homopolymer melt for which the model should work best and then to adjust the density of our semiflexible chain liquid so as to reproduce the long wavelength density fluctuations, or compressibility, of the real system. Since our model chain is linear, without branches, the "best case" is polyethylene (PE). In the melt state at 440 K, PE has a zero wavevector structure factor of $\hat{S}(k = 0) = \varrho_m k_B T \kappa_T \approx 0.25$,[50] where κ_T is the isothermal compressibility. *Ab initio* PRISM melt calculations using the realistic rotational isomeric state (RIS) model yield a slightly higher value. After having adjusted the bond bending energies in the more coarse-grained Koyama model to reproduce the aspect ratio of PE,[47] $\Gamma_{PE} \approx 1.2$, we found that a reduced density of $\varrho_m d^3 = 1.375$ is required to attain a value of $\hat{S}(k = 0) \approx 0.25$ based on the choice $l/d = 0.5$. This is consistent with the fact that real PE has a bond length of $l \approx 0.4d$ and a reduced density of $\varrho_m d^3 \approx 2$ due to a larger amount of methylene group overlap. On the other extreme, a melt density with a tangent bead chain ($l = d$) is $\varrho_m d^3 \approx 1$.

From the point of view of melt compressibility, there is a large degree of degeneracy in the mappings of coarse-grained models with different combinations of l/d and bond bending energies. From an intermolecular packing perspective, however, many of these models can be ruled out. One constraint on the model is to choose a bond length such that $l < d$. This leads to a lower accessible monomer surface area (compared to the tangent case) and, by definition, the chain will have more than one local length scale. These two features in a model lead to a very important, and rather general, feature of the *local* pair correlation function in real polymeric fluids: negative correlation, *i.e.* $g(r) < 1$ for *all* r. This is the result of two effects. First is the universal $1/r$ asymptotic approach of $g(r)$ to unity due to the long range correlation hole effect.[33,51] Second is the local, nonuniversal, structure which tends to be depleted even at melt densities. This effect has been seen in atomistic melt simulations of polyethylene,[52] polypropylene,[53] polystyrene,[54] and polyisobutylene.[55] It arises from the internal structure of a given chain having many different, but close in magnitude, length scales associated with bond length, bond angle, and dihedral angle constraints. This latter feature, coupled with the presence of thermal conformational disorder, leads to an interference effect which destroys strong solvation shells in the intermolecular pair correlation function as a result of averaging over all chain configurations. This local correlation hole is *not* seen either by theoretical means[48] or in simulation[56] at melt densities for the commonly employed tangent bead chain since essentially only one local packing length scale enters.

The motivation for choosing $l/d = 0.5$ is as follows. Using simple geometry, one can show that for a range

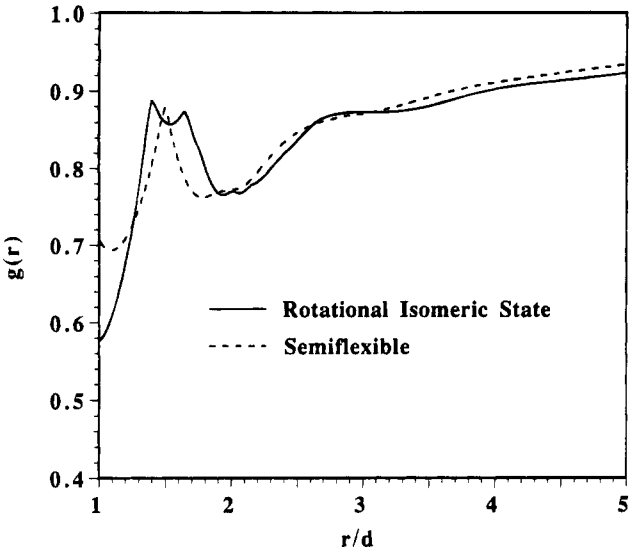

Figure 2. Homopolymer melt intermolecular site–site pair correlation functions. The solid line is a prediction for the pair correlation function of an $N = 6429$ polyethylene (PE) melt at $T = 440$ K. This is obtained by using the rotational isomeric state (RIS) model (see ref 50). To calibrate the density for the more coarse-grained semiflexible model used in this work, we fixed the isothermal compressibility to be $\beta\varrho_m\kappa_T = \hat{S}(k = 0) \approx 0.25$, which is nearly that of the real PE system. The resulting pair correlation function for an $N = 1000$ semiflexible chain melt of aspect ratio $\Gamma_{PE} \simeq 1.2$ is shown as the dashed line.

of hydrocarbon polymers the distance between the center of masses of repeat units along a backbone (e.g. a C_2H_4 unit for PE) is roughly half the effective diameter of the units themselves. Our use of an $l/d = 0.5$ overlapping site model does lead to melt pair distribution functions which *mimic* those determined by using a chemically realistic representation of a hydrocarbon chain such as the RIS chain, and hence of real systems.[47] An example of this is shown in Figure 2 for a homopolymer melt. This particular choice of parameters in the semiflexible chain depicted in Figure 1 (i.e. $l/d = 0.5$, and $\Gamma_A = \Gamma_B \equiv \Gamma_{PE}$ for the homopolymer case), along with a density of $\varrho_m d^3 = 1.375$, leads to a $g(r)$ which averages over some of the finer structure seen in the RIS melt, but has similar features. This appears to be the consequence of a strong correlation between the amplitude of long wavelength density fluctuations (compressibility) and local interchain packing in hard-core polymer fluids.[47] As we discussed in section II.C, for some questions it is only the integral over $g_{MM'}(r)$ which is relevant, and hence it is easy to see from Figure 2 how the more coarse-grained model (with carefully chosen parameters) would be sufficient.

The PRISM equations were solved numerically using the Picard iteration technique. This method involves initially satisfying the closure relation in real space and then enforcing the PRISM relations in Fourier transform space. Details of this procedure can be found in refs 17 and 35.

IV. Small-Angle Scattering

Generally, small-angle scattering experiments yield a weighted sum of the partial density–density fluctuation correlation functions. However, in many experiments the signal is often dominated by one of the components. In the case of small-angle X-ray scattering (SAXS) this is due to the disparity in electron density between the monomers in different components; in small-angle neutron scattering (SANS) measurements

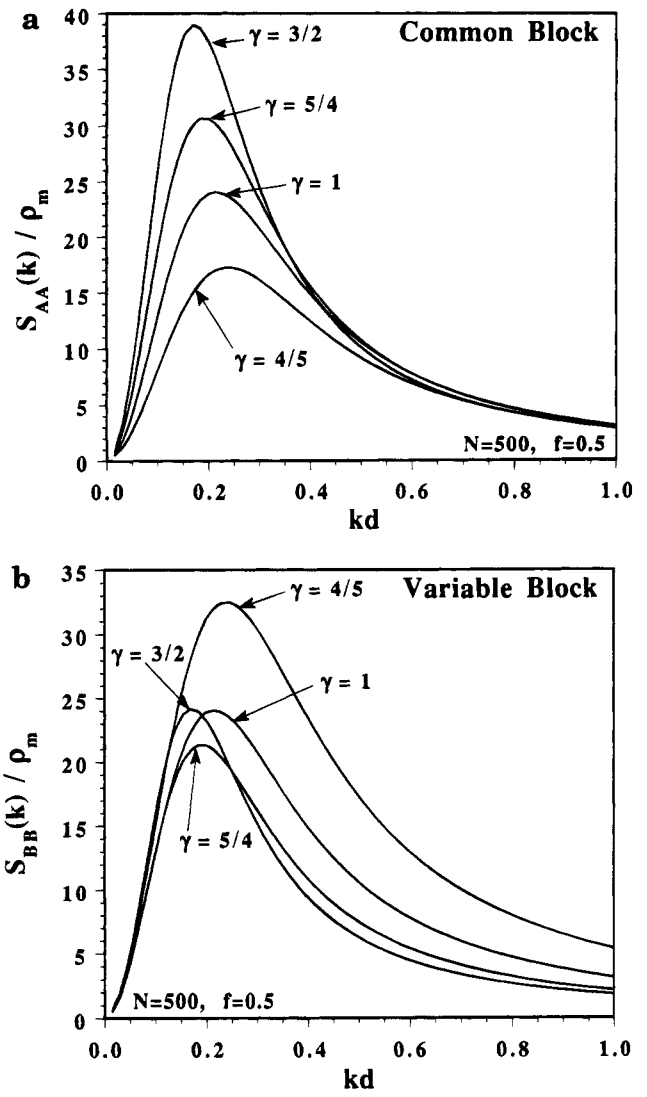

Figure 3. Low wavevector partial structure factors $\hat{S}_{AA}(k)$ and $\hat{S}_{BB}(k)$ at $N = 500$, $f = 0.5$ for copolymer models A–D. The common block structure factor (a) grows monotonically as the overall copolymer stiffness increases due to the increasing B-block aspect ratio. The variable block structure factor (b) varies nonmonotonically with its aspect ratio.

this arises as a result of selective deuterium labeling. Because most of the scattered intensity is often from one of the components, it is of interest to study the individual partial structure factors, $\hat{S}_{MM'}(k)$, and how they vary with stiffness disparity. Of course, in a hypothetical incompressible fluid there is only one unique structure factor, and this can be calculated within the IRPA[3] (modified to treat asymmetric architectures) in terms of a phenomenological χ parameter, or by *post-facto* enforcement of incompressibility within the PRISM theory.[17,57] For "effectively" athermal systems, which we are focusing on here, the bare enthalpic Flory interaction parameter is $\chi_o = 0$ [$v_{MM'}(r) = v(r) \neq 0$]. However, as we discuss later, non-zero effective thermal and athermal interaction parameters can be generated as a result of nonrandom mixing and finite melt compressibility.

Parts a and b of Figure 3 show the PRISM predictions for the small wavevector partial structure factors $\hat{S}_{AA}(k)$ and $\hat{S}_{BB}(k)$ for $N = 500$, $f \equiv N_A/N = 1/2$, and several stiffness disparity ratios $\gamma = \Gamma_B/\Gamma_A$ (see Table 1). Figure 3a shows how the "common block" structure factor, $\hat{S}_{AA}(k)$, is modified as a function of the variable

component (B-block) stiffness. This is relevant when the common block contributes most to the scattered intensity and where different B-blocks are attached to them. These peak intensities follow a monotonic trend with increasing *average*, or *overall*, copolymer stiffness. Since $k^* \propto 1/R_g$ the peak position moves toward a lower wavevector as the B-block stiffness increases, even though we are looking at the A-block scattering intensity. Although both partial structure factors have the same peak wavevector, the relative peak heights do change when we examine $\hat{S}_{BB}(k)$. Reflected in this quantity is how stable the B-block is to fluctuations of wavevector k and how this depends on its stiffness relative to the common block. As with $\hat{S}_{AA}(k)$, the overall scale is set by the average stiffness of the diblock copolymer. However, in contrast to the common block partial structure factor, the peak heights do not simply increase monotonically as γ becomes larger. Rather, the fluctuations in the variable component (B) depend on whether it is more or less rigid than the common block ($\gamma > 1$ and $\gamma < 1$, respectively). The variable block scattering function first decreases as it becomes less flexible, as seen in the curves of Figure 3b for $\gamma = {}^4/_5$, 1, ${}^5/_4$. Once γ is larger than unity (the B-block is stiffer than the common block), the variable component structure factor grows due to increasing *overall* block copolymer stiffness. As a general rule, the more flexible component has larger fluctuations, a conclusion consistent with recent constant volume Monte Carlo and PRISM calculations for athermal stiffness asymmetric *blends*.[58] This trend can be qualitatively understood for high densities and small wavevectors by the relation[16]

$$\hat{S}_{BB}(k) \approx \frac{\hat{C}_{AA}(k)}{\hat{C}_{BB}(k)}\hat{S}_{AA}(k) \qquad (4.1)$$

where for small wavevectors the direct correlation functions generally obey[16]

$$-\hat{C}_{\text{stiff-stiff}}(k) > -\hat{C}_{\text{flexible-flexible}}(k) \qquad (4.2)$$

as expected on the basis of the intuitive interpretation of $-k_BT\hat{C}_{MM'}(k = 0)$ as an effective repulsive pseudopotential strength between species M and M′. An alternative physical explanation is that microdomains composed of more flexible, poorly packed chains are less stable and hence exhibit larger long wavelength fluctuations.

Figure 4 further illustrates the general nonequivalence of the partial structure factors. Here we have plotted the chain length scaled reciprocal structure factors at peak wavevector, k^*, as a function of stiffness disparity, $\gamma = \Gamma_B/\Gamma_A$. Note that in the case of the common block $N/\hat{S}_{AA}(k^*)$ is a monotonic function of stiffness disparity, as discussed in relation to Figure 3a. On the other hand, the stability of the variable block passes through a maximum at a moderate value of stiffness. For either component, the deviations from the IRPA description (shown as the nearly horizontal solid line in Figure 4) suggest something about the sign of the effective χ parameters which could be extracted from these predictions. What we mean by the IRPA description is as follows. The IRPA structure factor is constructed using the same intramolecular distribution functions $\hat{\Omega}_{MM'}(k)$ employed in the PRISM calculation. Since the systems in this study are athermal, the χ_o term in $\hat{S}_{IRPA}(k)$ is identically zero and we simply have the "bare" structure factor,

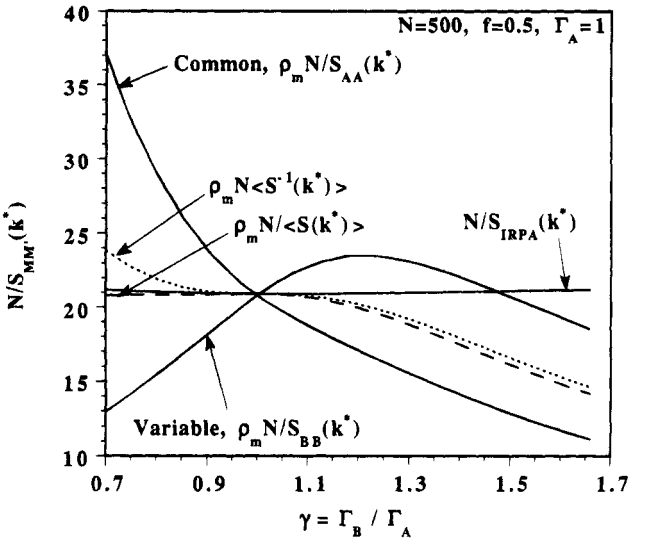

Figure 4. PRISM predictions for the reciprocal peak intensity of the partial structure factors and for the incompressible random phase approximation with $\chi_o = 0$ (see eq 4.3). The PRISM $\hat{S}_{AA}(k)$ and $\hat{S}_{BB}(k)$ are only equivalent for the special case of structurally symmetric copolymers and exhibit different dependencies on the block aspect ratio. Dashed lines are the averaged quantities $\langle\hat{S}^{-1}(k^*)\rangle$ (short dash) and $1/\langle\hat{S}(k^*)\rangle$ (long dash) discussed in the text.

$$\hat{S}_{IRPA}^{-1}(k) = \varrho_m \frac{\hat{\Omega}_{AA}(k) + \hat{\Omega}_{BB}(k) + 2\hat{\Omega}_{AB}(k)}{\hat{\Omega}_{AA}(k)\hat{\Omega}_{BB}(k) - \hat{\Omega}_{AB}^2(k)} \equiv \hat{S}_o^{-1}(k) \qquad (4.3)$$

As discussed above, the fluctuation correlations in the more flexible component are generally larger than those associated with the stiffer block. Over a fairly large range in γ, this leads to the flexible and stiff component structure factors to be greater and less than the IRPA prediction, respectively, for the same copolymer.

Using the PRISM predictions for the partial structure factors, we also define an effective χ parameter by

$$\chi_{ath}^{MM} \equiv \frac{1}{2}[\hat{S}_o^{-1}(k^*) - \varrho_m\hat{S}_{MM}^{-1}(k^*)] \qquad (4.4)$$

with the factor of ϱ_m being introduced to nondimensionalize the PRISM partial structure factors. Extracting effective χ parameters from these scattering functions using eq 4.4, we obtain net favorable and unfavorable interactions for the stiff and flexible components, respectively, for $\gamma \approx 1.45$ and lower. Above that point, *both* athermal χ parameters become positive. Listed in Table 2 are the values for χ_{ath}^{MM} as well as two species-independent, or "average", χ parameters defined by $2\bar{\chi}_{ath} \equiv [\hat{S}_o^{-1}(k^*) - \varrho_m\langle\hat{S}^{-1}(k^*)\rangle]$ and $2\chi_{ath} \equiv [\hat{S}_o^{-1}(k^*) - \varrho_m\langle\hat{S}(k^*)\rangle^{-1}]$. Note that χ_{ath} is literally the average of the partial χ parameters and hence corresponds to averaging the reciprocal intensity, whereas χ_{ath} derives from averaging the peak intensities first and then taking the reciprocal. More explicitly, the average denoted by the angled brackets is given by

$$\langle\hat{S}(k^*)\rangle \equiv \frac{1}{4}[\hat{S}_{AA}(k^*) + \hat{S}_{BB}(k^*) - 2\hat{S}_{AB}(k^*)] \qquad (4.5)$$

for the case of χ_{ath}. Similarly for $\bar{\chi}_{ath}$, we use the reciprocal partial structure factors. (In either case the minus sign is required to sum the *magnitudes* of the concentration fluctuations since $\hat{S}_{AB}(k^*) < 0$). Of course in experiments this quantity would generally involve a

weighted average since the scattering lengths of the monomers comprising the two blocks would differ. Note that a *single* χ parameter such as χ_{ath} contains no information regarding how the individual partial structure factors are deviating from the IRPA prediction. As seen from Figure 4, the IRPA prediction for the χ parameter at the spinodal is roughly $\chi_s N \approx 10.5$ (i.e. $2\chi_s N(f = 0.5, \gamma) \equiv N/S_{IRPA}(k^*) \approx 21$) and is virtually independent of γ over the range plotted. Comparing the value of $\chi_s(f = 0.5,\gamma) \approx 10.5/N$ to the χ parameters extracted from the PRISM calculations listed in Table 2, we find that the magnitude of the athermal contribution to the effective χ parameter is quite small. That is, $\chi_{ath}N \ll 10.5$, and hence the driving force toward microphase separation due to purely entropic packing considerations is quite small over this (usually) experimentally relevant range in γ.

In the limit of a very stiff B-block and a flexible A-block, such as the "rodcoil" diblock of Radzilowski, Wu, and Stupp,[59] the compressible PRISM theory predicts that the magnitude of each of the partial structure factors at peak wavevector is greater than or equal to that of the IRPA prediction. The start of this trend for modest asymmetries can be seen in Figure 4 for $\gamma \geq 1.45$, where both reciprocal peak intensities show a negative deviation from the IRPA, and hence positive χ parameters. However, we caution that our approach is best suited for applications to flexible and semiflexible diblocks, as we are only treating isotropically interacting units. For high aspect ratio polymers one must go beyond this approach, as anisotropic interactions and nematic-like orientational correlations are expected to become important.[6,10]

Finally, we would like to stress the importance of using a compressible description of the block copolymer fluid for calculating the collective structure factors. The assumption of incompressibility precludes the ability to extract information relating to individual components. Thus, even if one is interested in a single "net" χ parameter, without first studying the individual components it would be difficult to determine what factors control such a quantity in terms of physically relevant variables. However, for the range of aspect ratios covered in this study the athermal contribution is quite small relative to the thermal contribution (see section VI), and thus we do not want to overemphasize these deviations from the IRPA. Of course, the possibility of more dramatic (and larger in magnitude) departures from the IRPA is expected for the fully interacting systems (i.e. with the attractive tail branch of the interactions present). Issues related to the general nonequivalence of the partial structure factors, and how an effective χ parameter can be extracted in a meaningful way, have also been discussed by Dudowicz and Freed[5] within the lattice cluster theory description of copolymers and blends and by Tang and Freed[18] within compressible RPA theory.

V. Intermolecular Structural Correlations

A. Asymmetry and Chain Length Dependencies. The block-averaged intermolecular pair correlation functions, $g_{MM'}(r)$, characterize local, intermediate, R_g, and domain scale fluid structure. Related to these is $\Delta g(r)$ of eq 2.7 which describes the tendency for like monomers to pair at a distance r. We will focus on these two quantities in our discussion of the athermal system since the underlying local structure is what influences the effective thermal interactions through eq 2.11. We also note that the athermal reference pair correlation

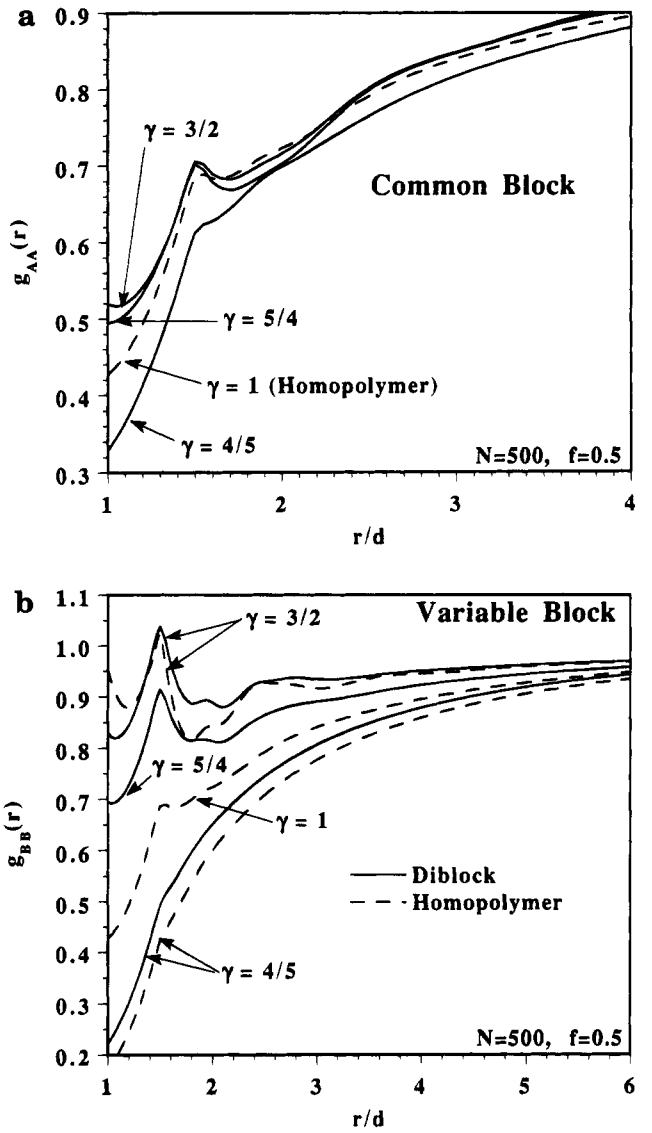

Figure 5. Diagonal block averaged intermolecular pair correlation functions $g_{AA}(r)$ (a) and $g_{BB}(r)$ (b) as a function of copolymer structural asymmetry for $f = 1/2$. The common component local packing increases slightly as the B-block stiffness is increased. The variable block packing is a strong function of copolymer stiffness since $g_{BB}(r)$ directly reflects B−B correlations. Shown as dashed lines are the homopolymer melt pair correlation functions for $N = 500$, where the chain aspect ratio is set to that of the B-block.

functions are required as input into PRISM theories for thermodynamics which separate the full interactions into repulsive hard-core and attractive tail branches.[39,60]

Parts a and b of Figure 5 show the diagonal pair correlation functions for stiffness asymmetric diblock melts for $N = 500$ and $f = 1/2$. Because stiffer chains tend to pack more efficiently, the following relation holds locally ($r \ll R_g$),

$$g_{\text{stiff-stiff}}(r) > g_{\text{flexible-flexible}}(r) \qquad (5.1)$$

Since the B-block stiffness in our calculations can be both higher and lower than that of the common block, relation 5.1 leads to

$$g_{BB}(r) > g_{AA}(r) \quad \gamma > 1, \text{ cases C, D} \qquad (5.2)$$

$$g_{BB}(r) < g_{AA}(r) \quad \gamma < 1, \text{ case A} \qquad (5.3)$$

Focusing on Figure 5a (the common block correlations), we see that the effect of grafting blocks of different flexibility onto a common block is to perturb the packing of that block relative to its homopolymer analog. If the B-block is more flexible than the common block (case A, $\gamma < 1$), it induces the common block to pack more like the flexible component. Likewise, attaching a B-block which is more rigid results in enhanced correlations between sites on the common block.

Figure 5b shows much larger effects since it is the stiffness of the B-block itself which is being varied. The change in $g_{BB}(r)$ with γ is akin to the change in the homopolymer $g(r)$ (dashed lines) with increasing stiffness.[48] It is these large changes in $g_{BB}(r)$ which give rise to the more modest changes in the packing between the common stiffness blocks seen in Figure 5a. This can be viewed as an "induced" structural rearrangement. For comparison, the dashed lines show the $N = 500$ homopolymer $g(r)$ using the aspect ratios corresponding to those in the B-block for a given choice of γ. Generally, the diblock pair correlation functions differ from the analogous homopolymer case in a way which brings them closer to that of the common block (more toward the $\gamma = 1$ case). Thus, just as the presence of the variable block *induces* changes in the local packing of the common block, the presence of the common block *suppresses* (with respect to the homopolymer) the amount by which the variable component packing changes as a function of aspect ratio. We note that the *direction* of the induced structural rearrangements seems to be nonuniversal. Recent calculations of short, structurally asymmetric, tangent-bead chain *blends*[58] indicate that the induced packing modifications upon blending can be in the opposite direction (i.e. $g_{MM}(r)$ move further apart) to those discussed here. To zeroth order, parts a and b of Figure 5 suggest that, *for modest overall diblock stiffness*, one can think of the common block as being somewhat unaffected by the presence of the other component. That very *assumption*, that the packing of the individual components in the pure state is similar to that in the mixed state, is implicit in the "regular solution" or "solubility parameter" description of the miscibility of blends and copolymers in terms of cohesive energy densities of the pure components.

Within the context of branching or side group effects, the degree of structural asymmetry depends on how branched the repeat units are. Crudely, the degree of branching translates into some effective backbone stiffness on an equal volume basis.[26,30,47] That is, the local packing described within a theory for a *branchless* polymer melt is representative of the packing in the real, branched chain fluid, provided that the correspondence between more branching and lower aspect ratio (and hence, less efficient packing) in the coarse-grained model is properly made. Although there are no explicit branches in our model, the effect of "shielding" the backbone sites due to increased branching translates into a decrease of the local $g(r)$ for more flexible blocks. The change of $g_{AA}(r)$ with increasing γ is interesting because it describes how the common block correlation functions are changed as a result of grafting increasingly "stiff" (or more lightly branched) blocks to it.

As mentioned previously, a single function which describes the degree of ordering in the fluid is $\Delta g(r)$ of eq 2.7. This quantity in the athermal limit arises solely from packing, and not from any unfavorable intermolecular interactions as discussed previously in the context of symmetric diblocks.[17] Remarkably, the magnitude of $\Delta g(r)$ is very small in comparison to the overall magnitude of the individual component $g_{MM'}(r)$. Figure 6 shows $\Delta g(r)$ for copolymers A–D ($\Delta g(r) = 0$ for case B due to perfect structural symmetry). Generally, the pairing amplitude monotonically increases with overall block stiffness. Although the magnitude is quite small, a $\Delta g(r)$ of order 10^{-2} can lead to appreciable thermal interaction energies, $\Delta\bar{E}$, since $\beta\epsilon$ is of order unity in the experimental temperature range. Although $\Delta\bar{E}$ is not literally a "χ parameter", it is a measure of the local energetic driving force for spatial segregation. Table 2 lists these values along with the athermal χ parameters discussed in section IV. As the copolymer asymmetry increases (with an average stiffness on either side of the symmetric copolymer "B"), $\Delta\bar{E}$ becomes larger. The magnitudes which come out of this simple calculation, after accounting for the "bare" interactions of methylene units ($\beta\epsilon \approx 1$ at 440 K on a 4 CH_2 basis), are large and consistent with the data on polyolefin alloys,[26,31] if we do associate this quantity with an effective thermal χ parameter. As discussed in section II.C, this connection between the "exchange energy" and the χ parameter is only well-defined in the blend (or perhaps for infinite N diblocks). Note that although the degree of nonrandom mixing and the overall stability of the fluid must be related, there is no obvious way in which $\Delta\bar{E}$ and χ_{ath} are correlated. Also note that the values of χ_{ath} are very small even relative to the mean field instability condition of $\chi \approx 10.5/N$ for $f = 1/2$. Thus, consistent with blend PRISM and Monte Carlo calculations[46,58] for structural asymmetries characteristic of flexible polymers, the purely athermal driving force toward phase separation appears very weak both in absolute terms and in relation to the thermal component (see also section VI).

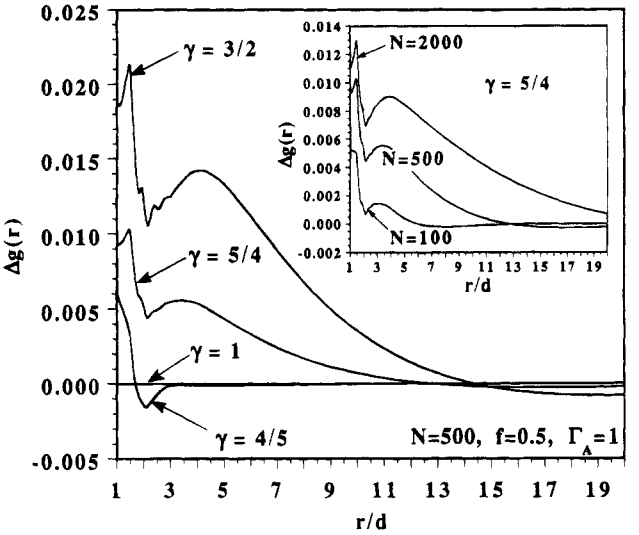

Figure 6. Difference function $\Delta g(r) \equiv 0.5[g_{AA}(r) + g_{BB}(r)] - g_{AB}(r)$ for $\gamma = 4/5$, 1, $5/4$, $3/2$ and $f = 1/2$. Larger deviations from random mixing are predicted as the stiffness disparity and/or the mean aspect ratio increases. The chain length dependence at constant asymmetry ($\gamma = 5/4$) is shown in the inset.

The intermolecular fluctuation quantity $\Delta g(r)$ generally increases with chain length, as seen in the inset of Figure 6. This result, however, is not general for all *types* of structural asymmetry. Our unpublished studies of asymmetric copolymers in which the size of the beads on two freely-jointed blocks was varied (i.e. $d_{AA} \neq d_{BB}$) show a trend in which $\Delta g(r)$, locally, saturates at a minimum value for large chain lengths.

Table 2. "Exchange Energy" $\Delta\bar{E}$ of Eq 2.11 in Units of $\beta\epsilon$ with Identical "Bare" Attractions (i.e. $v_{MM'}(r) \equiv v(r)$) for $f = 0.5$ and $N = 500$[a]

copolymer	γ	$\Delta\bar{E}/\beta\epsilon$	χ_{ath}^{AA}	χ_{ath}^{BB}	$\bar{\chi}_{ath}$	χ_{ath}	k^*d
A	4/5	0.031 06	−0.007 92	0.005 64	−0.000 87	0.001 96	0.239
B	1	0	0.000 119	0.000 119	0	0	0.215
C	5/4	0.080 88	0.000 468	−0.002 46	0.001 21	0.001 53	0.191
D	3/2	0.168 4	0.008 26	0.000 393	0.004 52	0.004 99	0.172

[a] The non-zero $\Delta\bar{E}$ arises as a result of nonrandom mixing of stiffness asymmetric copolymers. Also given are the peak positions k^*d and the athermal χ parameters discussed in the text.

Table 3. Chain Length Dependence of the Perturbative Estimate of the Dimensionless "Exchange Energy" $\Delta\bar{E}$ for Block Copolymer "C" ($\Gamma_A = 1$, $\Gamma_B = 5/4$) at $f = 0.5$[a]

	$\Delta\bar{E}/\beta\epsilon$	
N	diblock	blend
50		0.044 26
100	0.038 948	0.063 856
250		0.085 207
500	0.080 883	0.097 057
1000		0.105 71
2000	0.103 13	0.111 90

[a] Shown are values for the diblock ($N_A = N_B = N/2$) and the corresponding blend ($N_A = N_B = N$) under constant volume conditions.

The chain length dependence of $\Delta\bar{E}$ for this stiffness asymmetric model is given in Table 3, where we have also calculated the same quantity for the corresponding blend. Generally, the blend $\Delta\bar{E}$ is larger. This can be understood in terms of the local structure of the diblock versus the blend (not shown). The added constraint of a junction bond between the A and B chains suppresses the structural rearrangements in the diblock fluid. This leads to $\Delta g(r)$ being closer to zero (random mixing) than in the corresponding blend on the length scale of the interactions. Note that N in Table 3 is defined as $N = N_A + N_B$ and $N = N_A = N_B$ for the diblock and blend, respectively. For completeness, we have also included results for literally "snipping" the junction bond in the diblock, which corresponds to a blend of smaller chains. Table 3 also shows that $\Delta\bar{E}$ saturates for large N and the blend and copolymer results become closer. This is an indication that the thermal contribution to the effective χ parameter will approach a large N limit, as expected on general physical grounds.

B. Length Scale Dependent Compositions: Athermal *versus* Thermal Behavior. Deviations from random mixing are expected to play an important role in both material properties and the interpretation of dynamic measurements which probe the environment within a radius, R, of a given monomer. In data taken from nuclear magnetic resonance and dielectric spectroscopy (the "segmental" loss peak), R is believed to be a local length scale on the order of the monomer or segmental size.[41-45] Using the definition of eq 2.6, the consequences of nonrandom mixing in terms of an effective composition can be studied. Parts a and b of Figure 7 show $\Phi_{AA}(R)$ and $\Phi_{BB}(R)$ for copolymers A–D. By definition, in the thermodynamic limit of $R \to \infty$ the bulk composition is recovered. However, local and R_g scale structural fluctuations brought on by the conformational asymmetry can lead to either positive or negative departures from the bulk composition.

The common block composition $\Phi_{AA}(R)$ shown in Figure 7a indicates that the direction of the change locally from the bulk limit of $f = 1/2$ depends on whether this block is more or less flexible than the B-block. Generally, we find that enhancements in local composition occur for the more rigid component. Thus, when

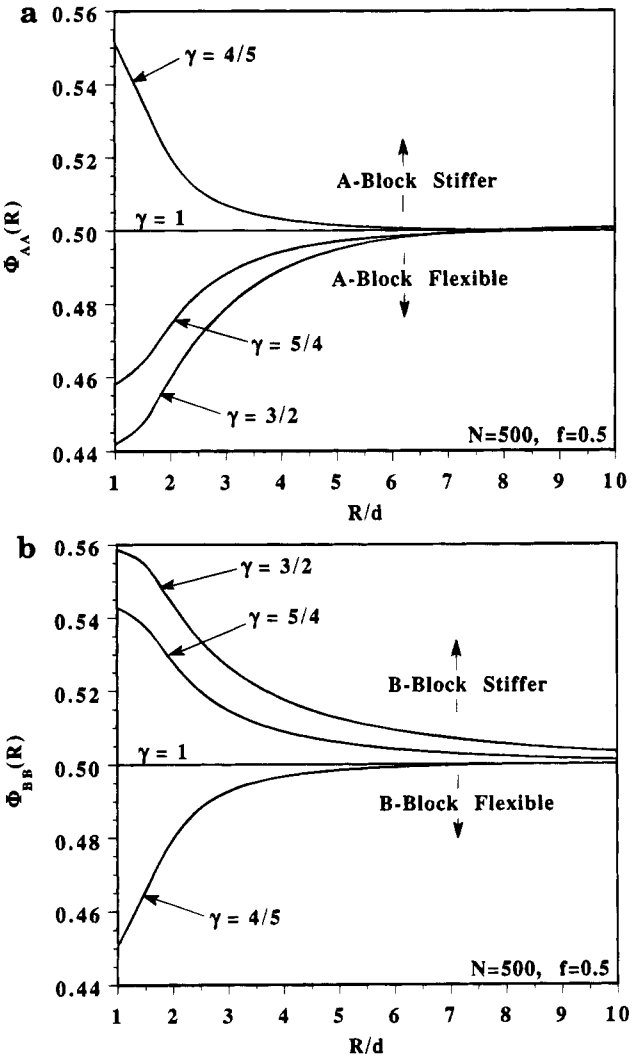

Figure 7. Effective intermolecular compositions $\Phi_{AA}(R)$ and $\Phi_{BB}(R)$ for $N = 500$, $f = 0.5$ diblocks having different stiffness mismatches. In this athermal limit, a small enhancement is predicted locally for the stiffer component, while the opposite is true for the more flexible component. Note here that once the temperature dependence of the local structure is explicitly accounted for, both $\Phi_{AA}(R)$ and $\Phi_{BB}(R)$ will be enhanced due to microdomain formation[17] (see Figure 8).

parts a and b of Figure 7 are compared for the A- and B-block local compositions, respectively, for each copolymer the stiffer block (whether it be A or B) obeys $\Phi_{stiff}(R) > f$, while for the other component $\Phi_{flexible}(R) < f$. Consistent with the change in magnitude of $\Delta g(r)$, the degree to which the local composition changes from the thermodynamic limit grows with increasing copolymer asymmetry and stiffness. The fact that for any given length scale, R, the compositions appear to obey the relation $\Phi_{AA}(R) + \Phi_{BB}(R) \approx 1$ may at first seem trivial on the basis of stoichiometric constraints. However, from the definition of eq 2.6 the *only* point at which this relation must hold rigorously is in the $R \to \infty$ limit

and/or under random mixing conditions of $g_{MM'}(r) \equiv g(r)$. In fact, previous calculations for structurally symmetric diblocks at low temperatures[17] with $v_{MM'}(r) \neq 0$, where there is a large degree of thermally-driven spatial segregation, show that *both* components can have large positive changes locally, thereby destroying this "conservation law" which we are discussing here for athermal diblock fluids.

The empirical fact that for these athermal systems we do find a nearly perfect conservation law for the local compositions suggests the relation

$$\Phi_{AA}(R) + \Phi_{BB}(R) = 1 + \Delta(R) \tag{5.4}$$

where $\Delta(R)$ is a measure of the degree to which a sort of "incompressibility"[40] on a particular length scale R holds. Using eq 2.6 for the definition of local composition, $\Delta(R)$ is easily determined,

$$\Delta(R) = \frac{f(1-f)[G_{AA}(R)G_{BB}(R) - G_{AB}^2(R)]}{[fG_{AA}(R) + (1-f)G_{AB}(R)][(1-f)G_{BB}(R) + fG_{AB}(R)]} \tag{5.5}$$

where

$$G_{MM'}(R) \equiv 4\pi \int_0^R dr\, r^2 g_{MM'}(r) \tag{5.6}$$

Thus, for a particular length scale, the "incompressibility" condition implies a geometric relation for the cross-correlation function,

$$\Delta(R) = 0 \rightarrow G_{AB}(R) = \sqrt{G_{AA}(R)G_{BB}(R)} \tag{5.7}$$

We emphasize that although this relation seems to hold fairly well, it *does not* mean that the literal assumption of incompressibility at the one-body level[40] should work well for these systems. As we discussed in the previous section, large deviations from the widely assumed incompressible relation $\hat{S}_{AA}(k) = \hat{S}_{BB}(k) = -\hat{S}_{AB}(k)$ are predicted for these copolymers. What eq 5.7 does indicate is that in the athermal limit, the cross-correlation function is closely related to the diagonal like–like species correlation functions in a manner reminiscent of the empirical Bertholet relation for Lennard-Jones interaction potentials.[35] Of course, the empirical Bertholet relation says nothing about the dependencies of pair correlation functions on stiffness asymmetry.

Although eq 5.7 seems to hold for the athermal systems shown in Figure 7, the additional presence of tail interactions leads to qualitatively different results, and much larger deviations from the bulk compositions. For comparison we have carried out calculations using the full PRISM copolymer theory[17] for the temperature dependent intermolecular correlation functions. Here, the copolymers interact through the repulsive hard core as well as a set of Lennard-Jones-like tail interactions. The symmetric tail interaction ordering employed previously[17] was used here: $v_{AA}(r) = v_{BB}(r) = 0$, $v_{AB}(r) > 0$.

Parts a and b of Figure 8 show $\Phi_{MM}(R)$ for $f = 0.5$ and $f = 0.1$, respectively, for the symmetric copolymer "B" ($\gamma = 1$) at several temperatures ($\chi_o \propto T^{-1}$) leading up to an "apparent spinodal", $(\chi_o N)_{S,App}(f)$.[61] Since $\gamma = 1$ corresponds to perfect structural symmetry, the athermal effective compositions are simply $\Phi_{AA}(R) = f$ and $\Phi_{BB}(R) = 1 - f$ (see Figure 7). However, as the temperature is decreased the repulsive AB tail interaction leads to strong composition fluctuations. For either composition, $\Phi_{MM}(R)$ approaches the pure component value of unity in the spatial region corresponding to the first solvation shell. For distances closer to the block size the effects are still appreciable. For example, at $\chi_o N = 10$ for $f = 0.5$, $\Phi_{AA}(R = R_{g,A}) \approx 0.6$ represents a 20% enhancement to the bulk limit. Near an apparent spinodal temperature[61] the deviations on the microdomain scale, $D \approx 3R_g$, are a few percent.

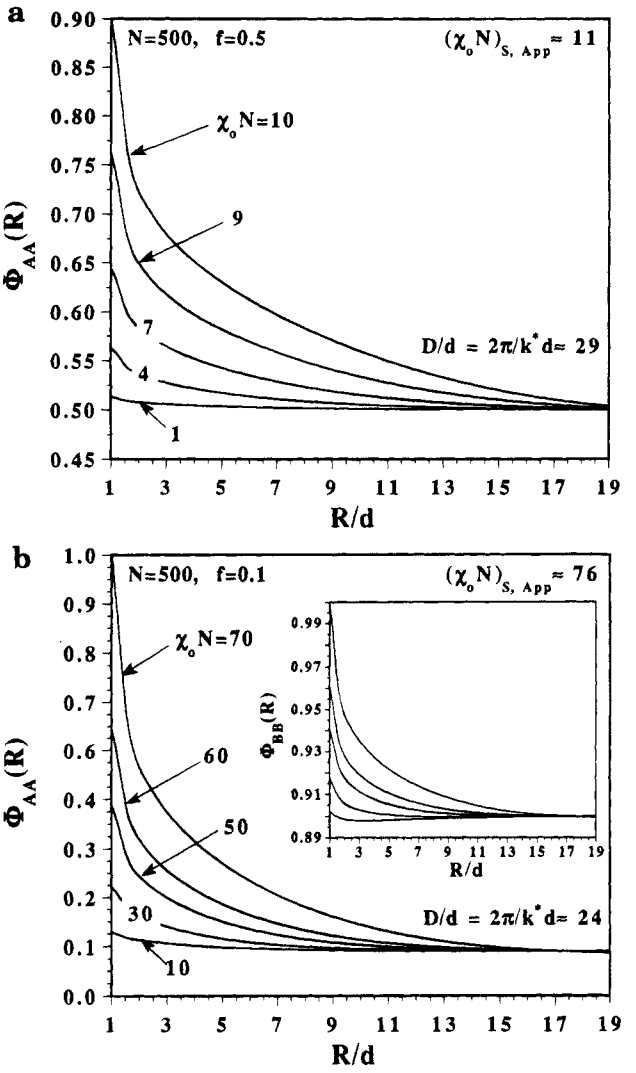

Figure 8. Effective intermolecular compositions for the structurally symmetric ($\gamma = 1$, copolymer "B") thermal diblock melt, with $N = 500$ and $f = 0.5$ (a) or $f = 0.1$ (b). For comparison to the purely athermal results of Figure 7, these quantities were calculated using the full PRISM theory for the temperature-dependent structural correlations (see ref 17), using a repulsive AB interaction $v_{AB}(r) > 0$ [$v_{AA}(r) = v_{BB}(r) = 0$]. Locally, the compositions become greater than the bulk values due to the AB spatial segregation which occurs as χ_o is increased. For reference, the block radii of gyration are $R_{g,A} = R_{g,B} = 6.4d$ for $f = 0.5$ and $R_{g,A} = 2.7d$, $R_{g,B} = 8.6d$ for $f = 0.1$.

Although we have only shown the structurally symmetric case, similar magnitudes are found for the thermal, structurally asymmetric models.[62] Noting the difference in the y-axis scales between Figures 7 (athermal) and 8 (thermal), we see the small negative and positive departures from random mixing in the athermal structurally asymmetric case will be "washed out" once the AB tail repulsion is present at finite temperatures. Regardless of the initial deviation of $\Phi_{MM}(R)$ due to pure

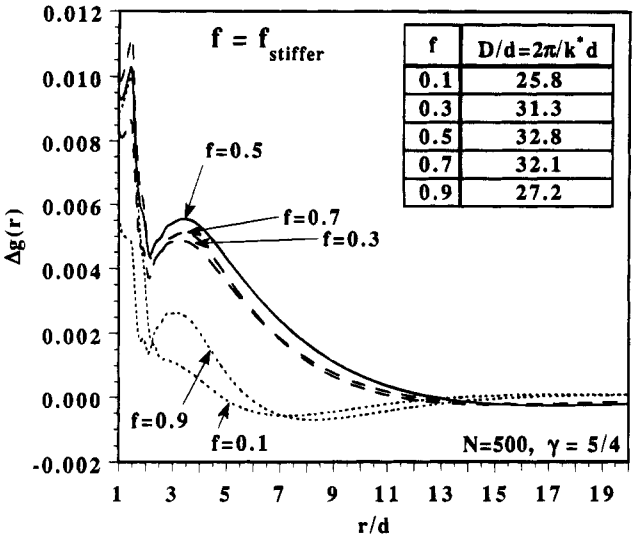

Figure 9. Composition dependence of $\Delta g(r)$ at $N = 500$ for model "C". This quantifies the degree to which deviations from random mixing occur, as well as the spatial extent of such deviations. Generally, $\Delta g(r)$ increases with increasing asymmetry and overall stiffness. Note that very locally ($r < 2d$) the ordering of $\Delta g(r)$ is as follows: $\Delta g(r; f = 0.3) > \Delta g(r; f = 0.7)$ and $\Delta g(r; f = 0.1) > \Delta g(r; f = 0.9)$, where $f \equiv f_{\text{stiffer}}$. The domain spacings $D \equiv 2\pi/k^*$ are listed in the inset.

structural asymmetries, we find that at finite temperatures $\Phi_{MM}(R)$ is always greater than its athermal value, and it eventually becomes greater than the bulk composition for *either* component. Hence eq 5.7 no longer holds for all length scales once explicit thermal effects are present. Physically, this arises from the depletion of AB contacts and "clustering" of like species as the fluid forms microdomains. Parts a and b of Figure 8 suggest that at low temperatures, both components experience local environments which are nearly pure in their respective species.

C. Copolymer Composition Dependencies. Shown in Figure 9 is $\Delta g(r)$ for copolymer C ($\gamma = {}^5/_4$) at $N = 500$ as a function of composition. Although the detailed structure is rather complicated locally, it is apparent that the overall deviations from random mixing decrease as the composition approaches either extreme for this particular γ. For this modest stiffness difference (although, roughly, it still covers the range of aspect ratios associated with the polyolefins[47]) they can be loosely grouped symmetrically about $f = {}^1/_2$. This, however, is slightly deceiving since much of the behavior for $r > 3d$ (the broad peak) is the result of these functions having different R_g scale periods of oscillation. Hence it is natural that, for instance, $f = 0.1$ and $f = 0.9$ look similar. Values for the "domain spacing" $D \equiv 2\pi/k^*$ are given in the inset of Figure 9. Generally, D becomes lower as the composition becomes more asymmetric (as in Leibler theory[3]). However, the values of D for $f_{\text{stiffer}} = 0.7$ and $f_{\text{stiffer}} = 0.9$ are slightly larger than their respective counterparts (i.e. $f_{\text{stiffer}} = 0.3$ and $f_{\text{stiffer}} = 0.1$) due to a larger *average* stiffness of the copolymer chain.

The quantities $\Delta\bar{E}$ and δH are more telling in terms of how the nonrandom mixing may affect the thermodynamic properties of the copolymer fluid. It is the subtle, nonuniversal monomer length scale structure in $\Delta g(r)$ which is relevant here, since the range of attractive interactions is on the scale of d, the hard-core diameter. Table 4 lists our perturbative estimate of $\Delta\bar{E}$ as a function of copolymer composition for the case

Table 4. Composition Dependence of $\Delta\bar{E}$ for Block Copolymer Models "A" ($\Gamma_A = 1$, $\Gamma_B = {}^4/_5$) and "C" ($\Gamma_A = 1$, $\Gamma_B = {}^5/_4$) for $N = 500$

	$\Delta\bar{E}/\beta\epsilon$	
f_{stiffer}	$\gamma = {}^4/_5$	$\gamma = {}^5/_4$
0.1	0.0490	0.0729
0.3	0.0371	0.0859
0.5	0.0311	0.0809
0.7	0.0231	0.0693
0.9	−0.000021	0.0397

shown in Figure 9 ($\gamma = {}^5/_4$) as well as for $\gamma = {}^4/_5$. Although both extreme compositions deviate less from random mixing for $\gamma = {}^5/_4$, the $\gamma = {}^4/_5$ case shows a monotonic trend in this composition range. This suggests that the trend in how a fluid deviates from random mixing depends not only on the *ratio* of block mismatch but also on the *average* stiffness of the chain. This nonuniversal dependence on *average* stiffness of the chain is also predicted for constant volume conformationally asymmetric polymer blends.[46]

The direction of the asymmetry in $\Delta\bar{E}(f)$ does show a systematic trend. In either case, when more of the flexible component is added, the local concentration fluctuations are greater in magnitude (e.g. for $\gamma = {}^5/_4$, $\Delta\bar{E} \approx 0.07$ for $f_{\text{flexible}} = 0.9$ versus 0.04 for $f_{\text{flexible}} = 0.1$). Physically, this arises due to the (constant density) fluid becoming more compressible as f_{flexible} is increased. In turn, the more compressible fluid *at a constant degree of mismatch* can more easily undergo structural reorganization. This argument is consistent with the predictions for both values of γ, but it must be emphasized that it seems to be valid only at constant γ. We should also emphasize our results are at constant volume, not pressure, and the influence of "equation-of-state" effects (a γ and f dependent density) is unknown at present within this approach. Using the lattice cluster theory, which is a thermodynamic description for constant pressure systems, Dudowicz and Freed[5] have addressed equation-of-state effects in the context of diblock melts.

VI. Estimates of Thermal Interaction Parameters

As discussed in section II.C, it is of interest to use the structural information from the athermal fluid in order to make perturbative estimates of the thermal contribution to an effective χ parameter. For copolymer fluids, the most unambiguous way to calculate a χ parameter is to perform an operation similar to what is done experimentally: treat the predicted structure factor as "data", and then fit it to an IRPA form. In copolymers, the periodicity of concentration fluctuations is finite, and hence the fitting procedure is done using $\hat{S}(k^*)$ rather than $\hat{S}(0)$ as in polymer blends. This procedure has been carried out for symmetric copolymers using the liquid state approach[17] but involves calculating the temperature dependence of $\hat{S}(k)$. Here we would like to perturbatively calculate a thermal "χ parameter" using the structural correlations in the athermal fluid. This will allow us to estimate the magnitude of the thermal contribution relative to the purely athermal contribution discussed in the previous section.

To do this, we must resort to using a description of the copolymer fluid at the thermodynamic level (i.e. $k = 0$). Since $k^* \sim 1/R_g$, using the "enthalpy of mixing" δH of eq 2.13 as a basis may be reasonable for large chain lengths. We have calculated the Flory-like quantity $\chi_H = \varrho_m^{-1}\delta H/f(1-f)$ as well as the second derivative

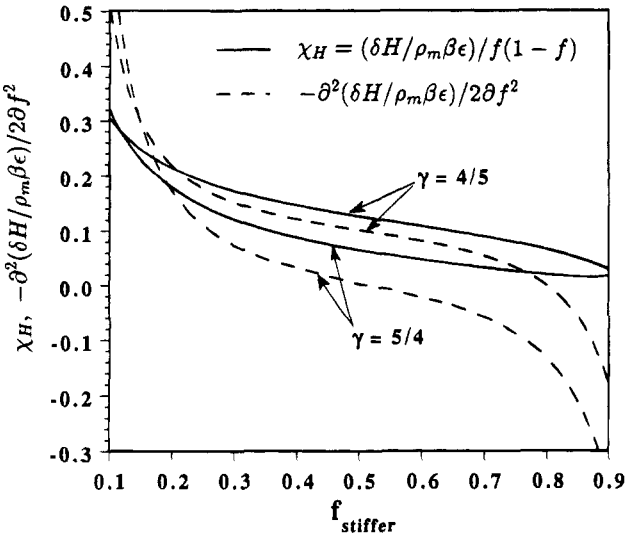

Figure 10. Thermodynamic perturbative estimates of the composition dependence of $\chi_H \equiv \varrho_m^{-1}\delta H/f(1-f)$ and $-\partial^2(\varrho_m^{-1}\delta H)/2\partial f^2$ for block copolymers "A" ($\Gamma_A = 1$, $\Gamma_B = {}^4/_5$) and "C" ($\Gamma_A = 1$, $\Gamma_B = {}^5/_4$) at $N = 500$. Numerical values for selected compositions are provided in Table 5.

of δH with respect to f. The latter of these is in direct analogy to the polymer blend, although it is unclear how this quantity is actually related to a χ parameter relevant to the microphase separation process. Figure 10 shows both quantities for $\gamma = {}^4/_5$ and $\gamma = {}^5/_4$. If this were a polymer *blend*, these two ways of calculating a χ parameter would converge, provided there were no appreciable composition dependence to the χ parameter, which would be true only if $g_{MM'}(r)$ were independent of composition. Since this is not generally true, and because f does not have the same physical meaning as ϕ, we do not necessarily expect $-\varrho_m^{-1}\partial^2(\delta H)/2\partial f^2$ to be close to χ_H. However, it is interesting that over a rather large range in composition both quantities exhibit a roughly linear dependence on f. In either case the composition dependence is nontrivial. As Tang and Freed[63] pointed out, a composition dependent χ parameter can lead to dramatic changes in the microphase behavior of diblocks. We therefore expect that the use of the liquid state theory predictions for the χ parameters in diblocks within a theory for the ODT and ordered phases may lead to considerable changes in the phase boundaries with respect to those results based on using a phenomenological composition-independent Flory χ parameter.

The level of consistency between χ_H and $-\varrho_m^{-1}\partial^2(\delta H)/2\partial f^2$ seems to be best for nearly symmetric compositions. For both values of γ the two quantities have the same dependence on f. The magnitude of χ_H for $\gamma = {}^5/_4$ is such that any small deviations can cause a sign change, and this turns out to be the case for the $f_{stiffer} > 0.5$ portion of the $-\varrho_m^{-1}\partial^2(\delta H)/2\partial f^2$ curve. Hence, the interpretation of this as a χ parameter for diblocks, in analogy with that for the blend, is probably not reliable for quantitative purposes.

Finally, the values for the "χ parameter" from Figure 10 are also listed in Table 5, and can be compared to $-\Delta\bar{E}$ in Table 4. Note that there is no unique correlation between these quantities. As we pointed out in section II.B, for the case of polymer blends, $-\Delta\bar{E}$ and $-\partial^2(\Delta H)/2\partial\phi^2$ will be close if the composition dependence of the pair correlation functions is sufficiently weak. For $f_{stiffer} \geq 0.5$ the estimated thermal χ parameters in Table 5 are large (since $\beta\epsilon \sim 1$ in the experimental temperature window) and much bigger than the corresponding athermal values in Table 2.

Table 5. Composition Dependence of $\varrho_m^{-1}\delta H/f(1-f)$ and $-\varrho_m^{-1}\partial^2(\delta H)/2\partial f^2$ for Block Copolymer Models "A" ($\Gamma_A = 1$, $\Gamma_B = {}^4/_5$) and "C" ($\Gamma_A = 1$, $\Gamma_B = {}^5/_4$) for $N = 500$

	$-(\partial^2/2\partial f^2)(\delta H/\varrho_m\beta\epsilon)$		$(\delta H/\varrho_m\beta\epsilon)/f(1-f)$	
$f_{stiffer}$	$\gamma = {}^4/_5$	$\gamma = {}^5/_4$	$\gamma = {}^4/_5$	$\gamma = {}^5/_4$
0.1	0.510	0.465	0.305	0.320
0.3	0.151	0.0528	0.171	0.120
0.5	0.101	0.00148	0.126	0.0645
0.7	0.0539	−0.0424	0.0891	0.0319
0.9	−0.181	−0.259	0.0283	0.0170

VII. Summary and Conclusions

In order to investigate the purely entropic driving force for microdomain formation in flexible diblock copolymer liquids, we have carried out calculations on model athermal, structurally asymmetric diblock melts. The use of PRISM integral equation theory, which has the ability to describe monomer packing on all length scales, is essential in order to characterize both local and long wavelength density and concentration fluctuations. Moreover, as discussed by both Dudowicz and Freed[5] and Schweizer and Curro,[16,34] compressibility effects even at high density are important with regard to the interpretation of scattering data. That is, in general, the three unique partial structure factors can be quite different from each other and can therefore lead to different estimates of the effective χ parameter, depending on which block dominates the scattering intensity. The most striking illustration of this is the general nonequivalence of the partial structure factors on the k^* scale (see Figure 4). This can lead to large differences (even sign changes!) in the value of an effective χ parameter, depending on which component is labeled and how χ is extracted.

In this work we also tried to assess the validity of using thermodynamic perturbation theory to calculate the enthalpic effective χ parameter. This approach only has a rigorous theoretical basis in the case of phase separating blends, where the wavevector of instability is $k = 0$, but for large N diblocks it may also be valid. Although we do not want to dwell on the precise values (due to the ambiguity in defining an enthalpy of mixing), there is clearly a composition dependence to the thermal χ parameter, and this could be significant when used in predicting the phase boundaries of such systems. We attempted this perturbative estimate to study an alternative, and much simpler, way of calculating the temperature dependent quantities based on the structural correlations in the athermal system and to compare the magnitudes of the thermal versus the athermal contributions to the χ parameter. Of course, for a direct (and more meaningful) comparison with experimentally determined χ parameters, it is much better to fit the predicted structure factors at peak wavevector based on PRISM theory which explicitly accounts for the tail potential modification of liquid structure. This method has been employed for symmetric copolymers,[17] but the calculations are numerically more involved than those presented here. Future studies will concentrate on extracting χ from the predictions of $\hat{S}^{-1}(k^*)$ versus $1/T$ for these asymmetric copolymers and comparing those results to the perturbative estimates presented in this paper and experimental measurements.[62] These more sophisticated methods also include "fluctuation stabilization" effects at low temperatures[17] which are neglected in a thermodynamic perturbative approach.

We have not predicted the phase behavior for diblock copolymer systems. Rather, we have investigated the relative stabilities of athermal melts of varying structural disparity [i.e. $\hat{S}(k^*)$ *versus* γ]. We have found that for a series of copolymers in which a common component is present, the local and longer wavelength correlations associated with this component can be altered by changing the conformational properties of the variable component. For example, the efficiency with which the subunits on the common block can pack can be adjusted by changing the conformational properties of the variable component. Of course, phase behavior of real copolymer and blend melts are often reported in terms of transition temperatures, even in the case of the polyolefins. Within PRISM theory based on the molecular closure schemes,[39] the study of the thermal phase stability requires as input these structural correlations in the athermal limit. Hence, our present work provides a starting point from which to investigate block copolymer thermal phase behavior.

In conclusion, our most important points can be summarized as follows: (i) Both the local and $1/k^*$ scale intermolecular properties of a *common* block can vary significantly depending on the characteristics of the block to which it is attached. This is seen as "induced" packing modifications in the athermal pair correlation functions of the common block and as a strong dependence of the common block collective structure factor on the stiffness of the second block. (ii) Non-zero *thermal* χ parameters can be generated as a result of nonrandom mixing at the local length scale. This suggests that even for systems having no net difference in interaction energies ($\chi_o \equiv 0$), segregation can still be enthalpically driven. This does not imply that excess entropic contributions to the χ parameter are not important, although they appear to be small relative to the critical χ values for aspect ratios typical of flexible polymers. Noncombinatorial entropic interactions are expected to play an important role for polymers with relatively large aspect ratios[9,46,58] and nematogens.[10] (iii) For conformationally asymmetric copolymers a *compressible* description of the liquid is essential. This is because both positive and negative deviations of the partial structure factors from the IRPA description are possible. (iv) Our predictions for the *athermal* diblock melt can best be tested by computer simulations of the *same model*. Comparison with experiments *assumes* the adequacy of the athermal model for describing the real fluid, an assumption which appears to be unreliable on the basis of our perturbative estimates of thermal contributions and prior PRISM analysis.[16,46] (v) Finally, we emphasize that for chain lengths relevant to experiment, explicit thermal effects or "clustering" manifested as temperature dependent intermolecular correlation functions and effective compositions may be very important and could have important consequences regarding the dynamics of such systems.

Acknowledgment. This work was supported by the National Science Foundation through the Materials Research Laboratory at the University of Illinois, Grant NSF-DMR-89-20538. E.F.D. also acknowledges partial support through a Program for Advanced Opportunities in Chemistry Fellowship. The authors are grateful to C. Singh, H. Tang, and K. Kolbet for their critical reading of the manuscript and useful suggestions.

Appendix A: Intramolecular Distribution Functions

The site–site intermolecular distribution functions, $\hat{\omega}_{\alpha M_\gamma M'}(k)$, for the discrete counterpart to the Koyama wormlike chain have been calculated by Honnell et al.[48] These functions are characterized by a bond bending energy, $E_b(r_{13})$, which is proportional to the cosine of the angle formed by three consecutive beads as shown in Figure 1, a bond length l, and a hard-core diameter d. From these parameters, it is straightforward to estimate the so-called aspect ratio, Γ, of the chain by equating the end-to-end distance of a Gaussian chain of the same length to that of the semiflexible model as in eq 3.2. Listed in Table 1 are those parameters used in this study.

The form for $\hat{\omega}_{\alpha M_\gamma M'}(k)$ needed to compute the intramolecular distribution function matrix, $\mathbf{\Omega}$, is given in ref 48 for homopolymers, and we make a simple extension of this for copolymers. Within a given block of species M, we have

$$\hat{\omega}_{\alpha M_\gamma M}(k) = \frac{\sin(B_M k)}{B_M k} e^{-A_M{}^2 k^2} \tag{A1}$$

where

$$A_M{}^2 = \frac{1}{6}(1 - C_M)\langle r_{\alpha M_\gamma M}{}^2 \rangle \tag{A2}$$

$$B_M{}^2 = C_M \langle r_{\alpha M_\gamma M}{}^2 \rangle \tag{A3}$$

$$C_M{}^2 = \frac{1}{2}\left(5 - 3\frac{\langle r_{\alpha M_\gamma M}{}^4 \rangle}{\langle r_{\alpha M_\gamma M}{}^2 \rangle^2}\right) \tag{A4}$$

The expressions for the second and fourth moments of the distribution are rather lengthy and are not reproduced here. The explicit formulas for these as functions of bond length, local bending energy, and $|\alpha - \gamma|$ can be found in ref 48. For the case of the off-diagonal elements, the quantity $\hat{\omega}_{\alpha A_\gamma B}(k)$ is approximated by the Markov product,

$$\hat{\omega}_{\alpha A_\gamma B}(k) = \hat{\omega}_{\alpha A N_A A}(k)\frac{\sin(kl)}{kl}\hat{\omega}_{N_A+1 B_\gamma B}(k) \tag{A5}$$

With use of this approximation, the double summation required to calculate $\hat{\Omega}_{AB}(k)$ can be rewritten as a product of single summations over homopolymer-like distribution functions.

References and Notes

(1) For a recent review see: Bates, F. S.; Fredrickson, G. H. *Annu. Rev. Phys. Chem.* **1992**, *41*, 525.
(2) Bates, F. S. *Science* **1991**, *251*, 898.
(3) Leibler, L. *Macromolecules* **1980**, *13*, 1602.
(4) Olvera de la Cruz, M.; Sanchez, I. C. *Macromolecules* **1986**, *19*, 2501.
(5) Dudowicz, J.; Freed, K. F. *Macromolecules* **1993**, *26*, 213. Freed, K. F.; Dudowicz, J. *J. Chem. Phys.* **1992**, *97*, 2105. Dudowicz, J.; Freed, K. F. *J. Chem. Phys.* **1994**, *100*, 4653.
(6) Holyst, R.; Schick, M. *J. Chem. Phys.* **1991**, *96*, 730.
(7) Kavassalis, T. A.; Whitmore, M. D. *Macromolecules* **1991**, *24*, 5340.
(8) Williams, D. R. M.; Fredrickson, G. H. *Macromolecules* **1992**, *25*, 3561.
(9) Fredrickson, G. H.; Liu, A. J.; Bates, F. S. *Macromolecules* **1994**, *27*, 2503. Bates, F. S.; Fredrickson, G. H. *Macromolecules* **1994**, *27*, 1065.
(10) Singh, C.; Goulian, M.; Liu, A. J.; Fredrickson, G. H. *Macromolecules* **1994**, *27*, 2974.

(11) Fredrickson, G. H.; Helfand, E. *J. Chem. Phys.* **1987**, *87*, 697.
(12) Olvera de la Cruz, M. *Phys. Rev. Lett.* **1991**, *67*, 85. Mayes, A. M.; Olvera de la Cruz, M. *J. Chem. Phys.* **1991**, *95*, 4670.
(13) Barrat, J.; Fredrickson, G. H. *J. Chem. Phys.* **1991**, *95*, 1281.
(14) Vilgis, T. A.; Benmouna, M. *Makromol. Chem. Theory Simul.* **1992**, *1*, 25.
(15) Muthukumar, M. *Macromolecules* **1993**, *26*, 5259.
(16) Schweizer, K. S. *Macromolecules* **1993**, *26*, 6033 and 6050.
(17) David, E. F.; Schweizer, K. S. *J. Chem. Phys.* **1994**, *100*, 7767 and 7784.
(18) Tang, H.; Freed, K. F. *Macromolecules* **1991**, *24*, 958.
(19) Yeung, C.; Desai, R. C.; Shi, A.; Noolandi, J. *Phys. Rev. Lett.* **1994**, *72*, 1834.
(20) Olmsted, P. D.; Milner, S. T. *Phys. Rev. Lett.* **1994**, *72*, 936.
(21) Matsen, M. W.; Schick, M. *Phys. Rev. Lett.* **1994**, *72*, 2660.
(22) Melenkevitz, J.; Muthukumar, M. *Macromolecules* **1991**, *24*, 4199. Lescanec, R. L.; Muthukumar, M. *Macromolecules* **1993**, *26*, 3908.
(23) Marie, P.; Selb, J.; Rameau, A.; Gallot, Y. *Makromol. Chem., Macromol. Symp.* **1988**, *16*, 301.
(24) Jung, W. G.; Fischer, E. W. *Makromol. Chem., Macromol. Symp.* **1988**, *16*, 281.
(25) Bates, F. S.; Rosedale, J. H.; Fredrickson, G. H. *J. Chem. Phys.* **1990**, *92*, 6255.
(26) Bates, F. S.; Schultz, M. F.; Rosedale, J. H.; Almdal, K. *Macromolecules* **1992**, *25*, 5547.
(27) Almdal, K.; Bates, F. S.; Mortensen, K. *J. Chem. Phys.* **1992**, *96*, 9122.
(28) Wolff, T.; Burger, C.; Ruland, W. *Macromolecules* **1993**, *26*, 1707.
(29) Floudas, G.; Vogt, S.; Pakula, T.; Fischer, E. W. *Macromolecules* **1993**, *26*, 7210.
(30) Gehlsen, M. D.; Bates, F. S. *Macromolecules* **1994**, *27*, 3611.
(31) Walsh, D. J.; Graessley, W. W.; Datta, S.; Lohse, D. J.; Fetters, L. J. *Macromolecules* **1992**, *25*, 5236. Graessley, W. W.; Krishnamoorti, R.; Balsara, N. P.; Fetters, L. J.; Lohse, D. J.; Schultz, D. N.; Sissano, J. A. *Macromolecules* **1994**, *27*, 2574. Graessley, W. W.; Krishnamoorti, R.; Balsara, N. P.; Butera, R. J.; Fetters, L. J.; Lohse, D. J.; Schultz, D. N.; Sissano, J. A. *Macromolecules* **1994**, *27*, 3896. Krishnamoorti, R.; Graessley, W. W.; Balsara, N. P.; Lohse, D. J. *Macromolecules* **1994**, *27*, 3073.
(32) Chandler, D.; Andersen, H. C. *J. Chem. Phys.* **1972**, *57*, 1930. Chandler, D. *Studies in Statistical Mechanics VIII*, Montroll, E. W., Lebowitz, J. L., Eds.; North-Holland: Amsterdam, 1982; pp 275–340.
(33) Schweizer, K. S.; Curro, J. G. *Phys. Rev. Lett.* **1987**, *58*, 246. Curro, J. G.; Schweizer, K. S. *J. Chem. Phys.* **1987**, *87*, 1842. Schweizer, K. S.; Curro, J. G. *Macromolecules* **1988**, *21*, 3070.
(34) Schweizer, K. S.; Curro, J. G. *Adv. Polym. Sci.* **1994**, *116*, 319.
(35) Hansen, J. P.; McDonald, I. R. *Theory of Simple Liquids*; Academic: London, 1986.
(36) Pratt, L. R.; Hsu, C. S.; Chandler, D. *J. Chem. Phys.* **1978**, *68*, 4202. Hsu, C. S.; Pratt, L. R.; Chandler, D. *J. Chem. Phys.* **1978**, *68*, 4213.
(37) Schweizer, K. S.; Honnell, K. G.; Curro, J. G. *J. Chem. Phys.* **1992**, *96*, 3211. Yethiraj, A.; Schweizer, K. S. *J. Chem. Phys.* **1992**, *97*, 1455. Melenkevitz, J.; Curro, J. G.; Schweizer, K. S. *J. Chem. Phys.* **1993**, *99*, 5571. Melenkevitz, J.; Schweizer, K. S.; Curro, J. G. *Macromolecules* **1993**, *26*, 6190. Grayce, C. J.; Schweizer, K. S. *J. Chem. Phys.* **1993**, *100*, 6846. Grayce, C. J.; Yethiraj, A.; Schweizer, K. S. *J. Chem. Phys.* **1994**, *100*, 6857.
(38) Chandler, D.; Singh, Y.; Richardson, D. M. *J. Chem. Phys.* **1984**, *81*, 1975.
(39) Schweizer, K. S.; Yethiraj, A. *J. Chem. Phys.* **1993**, *98*, 9053. Yethiraj, A.; Schweizer, K. S. *J. Chem. Phys.* **1993**, *98*, 9080.
(40) The length scale dependent effective compositions, $\Phi_{MM'}(R)$, are not to be confused with the one-body composition fields, $\phi_M(\mathbf{r})$, usually discussed in the context of polymer alloys. Those defined in eq 2.6 are the *inter*molecular contribution to the composition of species M′ inside a sphere of radius R centered around a site of type M. This is in contrast to the composition fields $\phi_M(\mathbf{r})$ which describe the composition of species M at a *point* in space $\mathbf{r}$. Thus when we use the term "incompressibility" in quotes in section V.B, this is not meant to be taken literally as the standard condition $\phi_A(\mathbf{r}) + \phi_B(\mathbf{r}) = 1$.
(41) Quan, X.; Johnson, G. E.; Anderson, E. W.; Bates, F. S. *Macromolecules* **1989**, *22*, 2541.
(42) Alig, I.; Kremer, F.; Fytas, G.; Roovers, J. *Macromolecules* **1992**, *25*, 5277.
(43) Stuhn, B.; Stickel, F. *Macromolecules* **1992**, *25*, 5306.
(44) Fytas, G.; Anastasiadis, S. H.; Karatasos, K.; Hadjichristidis, N. *Phys. Scripta* **1993**, *T49A*, 237.
(45) Chung, G.-C.; Kornfield, J. A. *Macromolecules* **1994**, *27*, 964.
(46) Schweizer, K. S.; Singh, C. *Macromolecules* **1995**, *28*, 2063.
(47) Schweizer, K. S.; David, E. F.; Singh, C.; Curro, J. G.; Rajasekaran, J. J. *Macromolecules* **1995**, *28*, 1528.
(48) Honnell, K. G.; Curro, J. G.; Schweizer, K. S. *Macromolecules* **1990**, *23*, 3496.
(49) Although PRISM theory is applicable over the entire range of densities, the Flory *ansatz* which we have adopted here is expected to be valid only for concentrated solutions and melt densities. Lower polymer concentrations and dilute solutions can properly be treated by relaxing the chain ideality assumption and calculating the intra- and interchain correlation functions self-consistently. See ref 37 for complete discussions of applying PRISM theory to polymer solutions. Moreover, even at melt densities the block segment lengths may be f dependent.
(50) Honnell, K. G.; McCoy, J. D.; Curro, J. G.; Schweizer, K. S.; Narten, A. H.; Habenschuss, A. *J. Chem. Phys.* **1991**, *94*, 4659.
(51) de Gennes, P. G. *Scaling Concepts in Polymer Physics*; Cornell University: Ithaca, NY, 1979.
(52) See, for example: Dodd, L. R.; Theodorou, D. N. *Adv. Polym. Sci.* **1994**, *116*, 249.
(53) Theodorou, D. N.; Suter, U. W. *Macromolecules* **1985**, *18*, 1467.
(54) Khare, R.; Paulaitis, M. E.; Lustig, S. R. *Macromolecules* **1993**, *26*, 7203.
(55) Han, J.; Boyd, R. H. *Macromolecules* **1994**, *27*, 5365.
(56) Curro, J. G.; Schweizer, K. S.; Grest, G. S.; Kremer, K. *J. Chem. Phys.* **1989**, *91*, 1357. Kremer, K.; Grest, G. S. *J. Chem. Phys.* **1990**, *92*, 5057.
(57) Schweizer, K. S.; Curro, J. G. *J. Chem. Phys.* **1989**, *91*, 5059.
(58) Weinhold, J.; Kumar, S.; Singh, C.; Schweizer, K. S. *Macromolecules*, to be submitted for publication. Singh, C.; Schweizer, K. S. *J. Chem. Phys.*, submitted for publication.
(59) Radzilowski, L. H.; Wu, J. L.; Stupp, S. I. *Macromolecules* **1993**, *26*, 879.
(60) Yethiraj, A.; Schweizer, K. S. *J. Chem. Phys.* **1992**, *97*, 5927.
(61) The PRISM theory for this system predicts a destruction of spinodal instabilities due to fluctuations. These effects are seen as nonlinearities in a plot of $\hat{S}(k^*)^{-1}$ versus $1/T$, and have been discussed elsewhere (see ref 17). For the purposes of discussing the proximity to the low-temperature fluctuation stabilization regime, we define an "apparent spinodal", $(\chi_o N)_{S,App}(f)$ as the point at which extrapolation of the linear, high-temperature portion of the $\hat{S}(k^*)^{-1}$ versus $\chi_o N$ curve crosses the $\chi_o N$ axis.
(62) David, E. F.; Schweizer, K. S. *Macromolecules*, to be submitted for publication.
(63) Tang, H.; Freed, K. F. *J. Chem. Phys.* **1991**, *94*, 7554.

MA946158J